

Introduction

Electromagnetic induction imaging (EMI) uses ultra-sensitive atomic magnetometers (AM), specifically radio-frequency atomic magnetometers (RF-AM). These devices are capable of detecting oscillating magnetic fields, making them ideal for EMI applications. The study aims to take experimental values for high-resolution EMI systems for various materials, focusing on the sensitivity and frequency range of the RF-AM. A single-channel rubidium RF-AM was developed, operating near room temperature with a sensitivity of 55 fT/Hz and a linewidth of 36 Hz, effective across the kHz-MHz band. The small sensor volume enhances spatial resolution. High-resolution EMI was demonstrated on materials with conductivities ranging from $6 \cdot 10^7 \text{ S m}^{-1}$ to 500 S m^{-1} , with sample volumes of a few cm^3 and an imaging resolution of around 1 mm. The feasibility of biomedical applications, such as imaging heart conductivity, will be done on the future (2 Mhz)

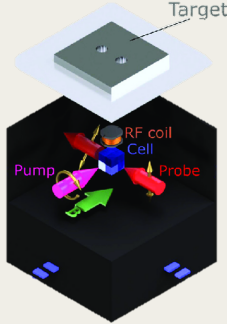


Figure 1. Probe and Pump Lasers, RF Coil in the portable atomic magnetometer

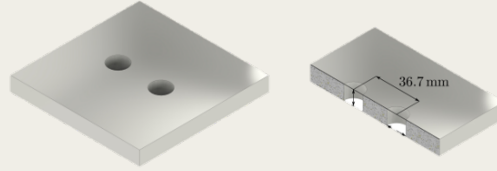


Figure 2. Sample with Two holes

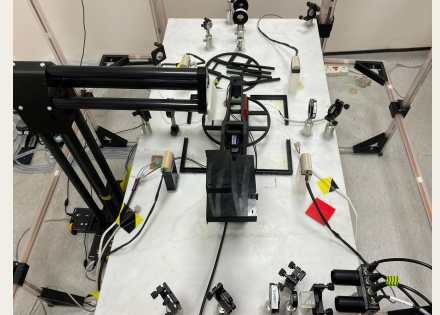


Figure 3. Experimental setup of the atomic magnetometer for induction imaging

In our study, we utilized an unshielded radio frequency-modulated atomic magnetometer (RF-AM) setup, based on the initial design by Savukov et al. (2005). At the core of the device is an alkali vapor cell containing rubidium (Rb), which is spin-polarized through optical pumping using a circularly polarized pump beam and a parallel DC magnetic field (bias field - BBIAS). The operating frequency of the RF-AM is adjusted via Helmholtz coils controlling the bias field, leveraging the Zeeman effect to suit the intended application. The magnetometer is calibrated using a known AC magnetic field, which induces a transverse atomic polarization rotation, measured by the rotation of a linearly polarized probe beam that crosses the pump beam perpendicularly. Detection is performed by a polarimeter equipped with a polarizing beam splitter and a balanced photodiode, with data analyzed using a lock-in amplifier and a spectrum analyzer.

Property 1: Electromagnetic induction imaging

In the setup described, the polarimeter, which consists of a polarizing beam splitter and a balanced photodiode (Thorlabs PDB210A), functions to detect the rotation of polarization in the probe beam. The rotation signal detected by the photodiode is then analyzed using a lock-in amplifier (LIA, Ametek 7280 DSP) and a spectrum analyzer (SA, Anritsu MS2718B).

- Oscillating magnetic field (primary field, B_1) induces Foucaults current response in a sample.
- Eddy current density depends on the sample's electromagnetic properties.
- Secondary response field (B_2) carries information regarding these properties.
- Phase-sensitive mapping of the total field produces images of the sample.

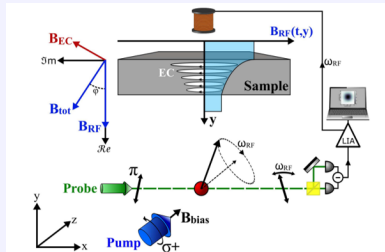


Figure 4. Principle of EMI, Circular polarisation for pump, linear polarisation for probe and pulsation by the Magnetic RF Field

Working conditions : Experimental photon

The described experimental conditions involve a 300 MHz Single Path Probe and Single Path Pump, operating in an environment controlled using optical modulation via Acousto-Optic Modulators (AOMs). RF sensitivity setting include a field strength of 2.05×10^{-12} . An additional RF parameter set at 0.1. The AOM for the pump is adjusted to 1.4 volts, and for the probe, it is set slightly higher at 1.6 volts. These voltages control the modulation of laser beams used in each path, affecting the frequency, intensity, and directionality of the lasers via sound waves generated within the AOM. We are operating at a temperature of 100 degrees Celsius.

Image processing Technics

The Gaussian filter smooths or blurs an image by applying a convolution with a Gaussian function, reducing noise while preserving overall structures. The degree of smoothing is controlled by the standard deviation σ , with larger σ leading to more blurring. Convolution, used to apply filters, combines the image and filter through summation of their products. Cubic interpolation estimates values between data points. An algorithm can calculate the distance between two holes, tested using a small magnetometer on target data.

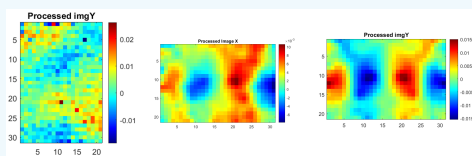


Figure 5. Raw data, Gaussian filtering, and gradient remover

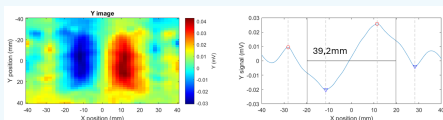


Figure 6. Two holes distance calculation, data fusionning on a centering band

Lortezian feating function : Processing of experimental values

The given algorithm outlines a method for fitting Lorentzian curves to data points, which is particularly useful in the context of atomic magnetometry for interpreting magnetic resonance signals. The algorithm processes multidimensional input data and applies Lorentzian and derivative models to each pixel. This allows for a detailed analysis of the lineshapes of the transverse spin components, represented as \tilde{S}_x and \tilde{S}_y , in a magnetic field. The Lorentzian lineshape for the \tilde{S}_x component is described by the formula:

$$\tilde{S}_x(\omega_{RF}) = S_0 B_{RF} \gamma \frac{\Gamma}{4[(\omega_{RF} - \Omega_L)^2 + \Gamma^2/4]},$$

which is centered on the Larmor frequency Ω_L with a linewidth Γ indicating the system's sensitivity. This response is important for determining the properties of the magnetic field by analyzing the detected frequency shifts. Similarly, the dispersive component, \tilde{S}_y , which provides complementary information about the magnetic field dynamics, is given by:

$$\tilde{S}_y(\omega_{RF}) = S_0 B_{RF} \gamma \frac{(\Omega_L - \omega_{RF})}{2[(\omega_{RF} - \Omega_L)^2 + \Gamma^2/4]},$$

The algorithm involves initializing parameters, performing least-squares optimization to match the Lorentzian model to the observed data accurately, and optionally displaying the results through plots. This method is invaluable in refining our understanding of magnetic fields and enhancing the sensitivity and performance of magnetometers in applications such as medical imaging and geophysical exploration.

$$\Gamma = \frac{2}{T_2} \sqrt{1 + \frac{\gamma^2 B_0^2 T_1 T_2}{4}},$$

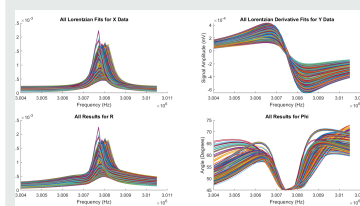


Figure 7. Lorentzian fitting results for our experimental data (Circular copper)

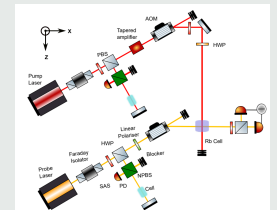


Figure 8. Probe, pump for the laser lightpath. Lightpath controlled with a probe and pump AOM

Imaging results for a copper coin

The LIA processes the signal to extract four key streams of data: the in-phase (absorptive, labeled as X) and out-of-phase (dispersive, labeled as Y) components of the polarimeter's output. Additionally, it calculates the radius $R = \sqrt{X^2 + Y^2}$ and the phase $\Phi = \arctan\left(\frac{Y}{X}\right)$. These outputs (X , Y , R , and Φ) along with the spectral traces from the SA are then recorded on a laptop for further analysis and interpretation. This setup allows for detailed and precise measurements of the polarization properties of the probe beam, which are important for applications in fields such as quantum computing, magnetic field sensing, and optical analysis.

